

## Precise STM spectroscopy on the superconducting phase of $\text{Bi}_2\text{Sr}_2\text{CaCu}_2\text{O}_8$

This article has been downloaded from IOPscience. Please scroll down to see the full text article.

1995 J. Phys.: Condens. Matter 7 L545

(<http://iopscience.iop.org/0953-8984/7/42/001>)

View [the table of contents for this issue](#), or go to the [journal homepage](#) for more

Download details:

IP Address: 171.66.16.151

The article was downloaded on 12/05/2010 at 22:17

Please note that [terms and conditions apply](#).

## LETTER TO THE EDITOR

# Precise STM spectroscopy on the superconducting phase of $\text{Bi}_2\text{Sr}_2\text{CaCu}_2\text{O}_8$

Koichi Ichimura†, Koji Suzuki†, Kazushige Nomura† and Shunji Takekawa†

† Department of Physics, Hokkaido University, Sapporo 060, Japan

† National Institute for Research in Inorganic Materials, Tsukuba, Ibaraki 305, Japan

Received 7 August 1995

**Abstract.** We carried out electron tunnelling spectroscopy for single crystals of  $\text{Bi}_2\text{Sr}_2\text{CaCu}_2\text{O}_8$  in the superconducting phase with use of STM. The tunnelling differential conductance curve with low noise was obtained for the cleaved surface and compared with that for the lateral surface. The two spectra were found to be essentially identical. It is concluded that tunnelling spectra obtained by our STM experiment contain contributions from every wave number and represent the total electronic density of states. From the functional form of the tunnelling conductance, the simple d wave was excluded for the symmetry of the superconducting pair wave function. The conductance curve obtained was well explained by the model, in which the gap is finite on the whole Fermi surface while it is highly anisotropic in  $k$ -space. It was suggested that the symmetry of the superconducting pair wave function is of the mixed symmetry of the s and d waves.

The determination of the symmetry of the pair wave function is very important in elucidating the mechanism of superconductivity. It is known that in high- $T_c$  oxides the superconductivity is brought about by carriers in the Cu–O layer where the Coulomb repulsive interaction is fairly strong. The d-wave symmetry has been discussed as a possible symmetry for the attractive interaction in such a strong-correlation system. In order to investigate the pair symmetry many kinds of experiments have been done, e.g. measurement of the magnetic field penetration depth [1], angle-resolved photoemission spectroscopy [2], NMR relaxation rate measurement [3]. Among these experiments electron tunnelling spectroscopy, in which the electronic density of states is rather directly obtained, is most favourable for determining the symmetry of the pair wave function. The scanning tunnelling microscopy (STM) method, in which the tunnelling barrier can be controlled microscopically, is useful for an investigation of high- $T_c$  oxides with layered structure.

Since the discovery of high- $T_c$  oxides, many tunnelling experiments have been carried out. Recently, the in-plane anisotropy of tunnelling spectra, which has been reported in experiments using STM [4, 5], and the gap anisotropy observed in tunnelling spectroscopy have been attracting much interest. We have also reported from experiments using STM spectroscopy for the lateral surface of  $\text{Bi}_2\text{Sr}_2\text{CaCu}_2\text{O}_8$  [6] that the gap is infinite on the Fermi surface while it varies depending on the direction in  $k$ -space. However, the tunnelling current at the lateral surface was not completely stable and the conductance curve obtained was slightly noisy because of unstable surface conditions, partly due to the metallic nature of the Cu–O layer directly exposed to the lateral surface. In order to obtain the precise functional shape of the tunnelling conductance, we investigated the cleaved surface of single crystals of  $\text{Bi}_2\text{Sr}_2\text{CaCu}_2\text{O}_8$ , in which more stable measurement was possible as

compared with the lateral surface, with use of low-temperature STM. In this letter, we present tunnelling data with low noise and discuss the symmetry of the pair wave function.

Single crystals of  $\text{Bi}_2\text{Sr}_2\text{CaCu}_2\text{O}_8$  used in the measurement were grown using the floating-zone method. The superconducting transition temperature  $T_c$  was determined as  $T_c = 87$  K from the midpoint of the resistive transition. The clean surface was obtained by cleaving along the  $a$ - $b$  plane. In order to maintain a clean sample surface, the sample was mounted in the STM cell unit immediately after cleaving. The cell was first evacuated and then filled with thermal exchange helium gas. Mechanically sharpened Pt-Ir wire was used as the STM tip for spectroscopic measurement.

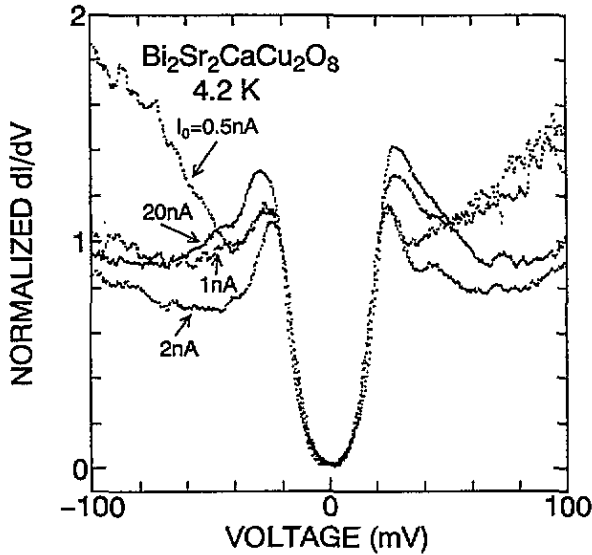


**Figure 1.** The tunnelling differential conductance obtained at the cleaved surface of the single crystal for various tip distances. The tip distance from the sample surface is characterized by the initial tunnelling current  $I_0$  at the constant bias voltage  $V = 100$  mV. Curves for  $I_0 = 0.5$ , 1, 2 and 20 nA at  $V = 100$  mV are shown together, normalized at  $V = 20$  mV.

Figure 1 shows the tunnelling conductance obtained at the cleaved surface for various tip distances from the sample surface, which are characterized by the initial tunnelling current  $I_0$  at constant bias voltage  $V = 100$  mV at 4.2 K. Each curve is normalized at  $V = 20$  mV. It should be noted that the noise in the tunnelling conductance spectra has been much reduced as compared with those in our previous measurements. As shown in the figure, the energy gap structure associated with the superconducting state is clear. However, the total tunnelling spectra vary depending on the tip distance, identically to the previous result [7]. The tip distance dependence of the conductance curve was confirmed to be reproducible at fixed positions. It assures a non-contacting tip configuration to the sample surface. For a large tip distance, the differential conductance increases with the bias voltage outside the gap edge and shows the so-called V-shape as is reported frequently [8]. On the other hand, for relatively small tip distance the conductance curve does not show the V-shape and becomes rather flat outside the gap edge. At any tip distance, our tunnelling spectra are not asymmetric, unlike those in the recent paper [9]. Contrary to in the region outside, the conductance curve inside the gap is essentially the same irrespective of the tip distance.

Metallic electrons are confined within the Cu-O layer in high- $T_c$  oxides and the surface layer is the Bi-O layer for the cleaved surface. Accordingly, the tunnelling current flows through the tunnelling barrier which consists of insulating Sr-O, Bi-O and the vacuum gap in series. The tunnelling matrix element  $|M|$  is likely to depend on the energy for such a complicated tunnelling barrier [7]. The variation of width of the vacuum gap, which corresponds to the tip distance, modifies the energy dependence of  $|M|$ . However,  $|M|$  is deduced to be approximately constant in the low-energy region. It is considered that the tunnelling conductance obtained for the cleaved surface correctly represents the electronic density of states of the sample in the low-energy region as that for the lateral surface which is proportional to the electronic density of states over wider range [6]. Accordingly, we only discuss below the differential conductance inside the gap edge.

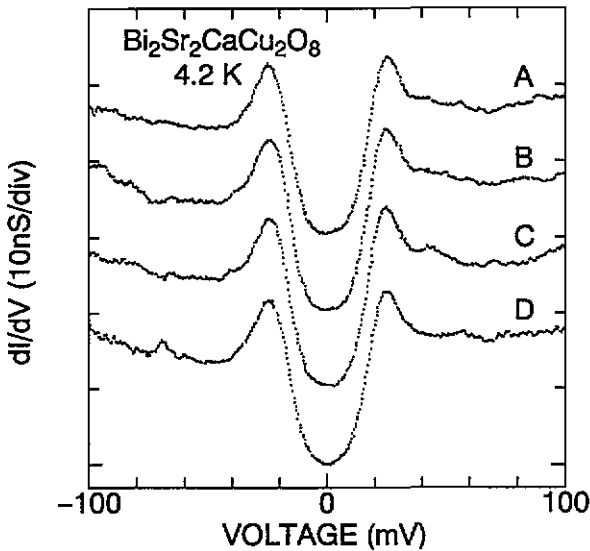


**Figure 2.** The differential conductance at various positions on the surface for  $I_0 = 2$  nA at  $V = 100$  mV. A, B, C and D are aligned in order and at intervals of about 10 nm. The zero-conductance line of each curve is shifted by one division for clarity.

Figure 2 shows the tunnelling differential conductance at various positions on the sample surface. Positions A, B, C and D are aligned in order and at intervals of about 10 nm. Essentially the same curve is reproduced irrespective of the position on the surface, while small variation is found. For A, B and C, the differential conductance shows a flat behaviour in the low-bias voltage region. However, the conductance at position D shows  $E^2$ -dependence near zero-bias voltage. The  $E^2$  dependence was sometimes observed for different samples. In such cases, the zero-bias conductance is slightly larger, suggesting the broadening of the one-electron level. It is deduced that the broadening of the one-electron level is locally larger at D as compared with A, B or C. The position dependence of the conductance curve is presumably attributed to some kind of inhomogeneity which leads to variation in the lifetime broadening effect. Accordingly, the curves for A, B or C represent the intrinsic feature with less broadening effect. We will discuss the tunnelling spectrum for C below in detail.

In figure 3 we compare the conductance curve obtained at C on the cleaved surface (solid line) with that for the lateral surface (broken line) obtained in previous measurements

[6]. Although the gap value is slightly different, these spectra show essentially identical functional forms. In a simple model, the transition probability of electron tunnelling depends on the component of the kinetic energy of the tunnelling electron perpendicular to the tunnelling barrier, and its dependence is described by the factor  $\exp(-\beta \sin^2 \theta)$ , where  $\theta$  is the angle between the wave number vector and the normal to the tunnelling barrier and  $\beta$  is the constant given as [10]

$$\beta = \sqrt{\frac{2m}{\hbar^2}} \frac{E_F}{\sqrt{U - E_F}} d \quad (1)$$

where  $U$  and  $d$  are the potential height and the width of the tunnelling barrier, respectively. Such a model suggests that angle-resolved measurement is possible by electron tunnelling spectroscopy in the case where  $\beta$  is substantially large. For a typical tunnelling junction with an area of  $10^{-5}$  cm<sup>2</sup> and a resistance of 30  $\Omega$ ,  $\beta$  is roughly estimated as  $\beta \sim 20$  [11]. In this case, the transition probability decays by a factor of  $e^{-1}$  at  $\theta = 13^\circ$ . Actually, the gap anisotropy for lead was measured for tunnel junctions formed along various crystal orientations [12].

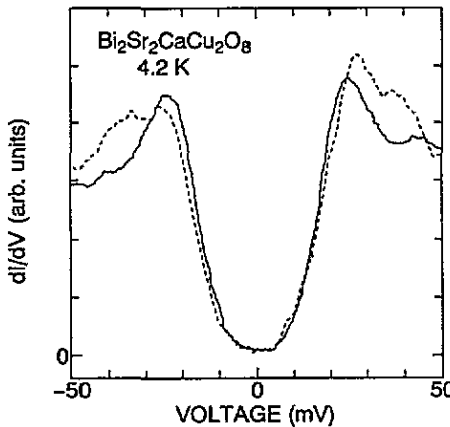


Figure 3. The differential conductance for the cleaved surface (solid line) compared with that for the lateral surface (broken line) reported previously [6].

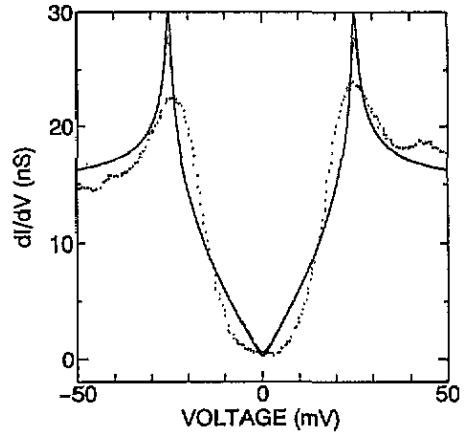


Figure 4. Fitting of the conductance obtained to the d-wave model. The solid line represents the calculated conductance for 4.2 K from the d-wave anisotropy of the gap with  $\Delta_0 = 25$  meV. The broken line represents the broadened curve of the solid line with  $\Gamma = 0.25$  meV.

The Fermi surface of high- $T_c$  cuprates is regarded as two dimensional. There is little dispersion along the  $k_z$ -direction. Naïvely, it is considered that the tunnelling electron which carries the current along the  $c$ -axis contains every wave number component in the  $k_x$ - $k_y$  plane with equal weight. It has been well established that the metallic electrons which bear the superconductivity are confined within the two-dimensional Cu-O layer and that the gap anisotropy is in the  $k_x$ - $k_y$  plane. If angle-resolved tunnelling spectroscopy is possible, the tunnelling spectrum at the cleaved surface would be quite different from that at the lateral surface. However, the present results show that there is no difference in tunnelling spectra between the cleaved ( $I \parallel c$ -axis) and the lateral surface ( $I \parallel a$ -axis). This fact indicates that the present STM method does not probe electrons with a particular wave number but

the total sum practically in  $k$ -space, in contrast to the claim of Kane *et al* [4], presumably because the  $\beta$  value is rather small. In the nearly square lattice of the Cu-O layer, the gap is expected to be of fourfold symmetry. The value of  $\beta = 2$ , in which the transition probability decays by a factor of  $e^{-1}$  at  $\theta = 45^\circ$ , practically averages out every component of the wave number. For  $\beta = 2$ , the tip distance  $d$  is roughly estimated as  $d \sim 0.2$  nm, where the Fermi energy  $E_F$  and the work function  $\Phi = U - E_F$  are assumed to be 4 and 5 eV, respectively. The tip distance of about 0.2 nm seems to be somewhat small. However, the above estimation is very crude and  $\beta = 2$  is not inconsistent with the actual experimental conditions. It is concluded that tunnelling spectra at both the cleaved and the lateral surface practically contain contributions from the whole wave number. Therefore, our present result obtained at the cleaved surface should be recognized as corresponding to the total density of states as in our previous results, obtained at the lateral surface.

The tunnelling differential conductance obtained clearly shows the energy gap structure. The differential conductance is reduced to almost zero and is flat near zero-bias voltage, similarly to the BCS density of states with s-wave pairing symmetry. On the other hand, finite conductance appears inside the gap edge. Such a finite conductance cannot be explained by the BCS density of states, even if the broadening of the one-electron level is taken into account. This strongly suggests gap anisotropy. We try to fit the data to the electronic density of states for anisotropic gap models.

Firstly, we discuss the d-wave symmetry with line nodes of the gap  $\Delta$ . The d wave is examined with the most simple form as

$$\Delta(k) = \Delta_0 \cos(2\phi) \quad (2)$$

where  $\Delta_0$  is the amplitude of  $\Delta$  and  $\phi$  is the azimuth. For the sake of simplicity, we assume that the band dispersion is isotropic. Details of these calculations have been described in our previous article [6]. Since the tunnelling spectrum obtained is given practically by the total sum of every wave number as discussed above, it may be compared with the total density of states which is calculated by integrating over all directions in  $k$ -space. The calculated differential conductance for 4.2 K with  $\Delta_0 = 25$  meV is shown in figure 4 as the solid line. It is proportional to the energy in the low-energy region. The broken line in figure 4 is the broadened curve of the solid line with the broadening parameter  $\Gamma = 0.25$  meV. A small  $\Gamma$  value increases the conductance near zero-bias voltage, while the energy dependence is still almost linear. A calculation for realistic band structure, in which the Fermi surface is of the half-filled band in a two-dimensional tight-binding approximation for a simple square lattice [13], is also possible. It only decreases the slope at low-energy region by about 30% at most. The linear dependence on energy is a general feature of the d-wave anisotropy with line nodes of the gap. It is obvious that the measured conductance is almost flat near zero-bias voltage and cannot be explained by the pure d-wave pairing, even if we take both the realistic band dispersion and the broadening effect into account. It is clear that the gap is finite on the whole Fermi surface.

We examine another anisotropic model with finite gap, in which  $\Delta$  varies depending on the direction in  $k$ -space. We introduce the gap density function of a rectangular form as [6]

$$D(\Delta) = \begin{cases} \frac{1}{\Delta_{\max} - \Delta_{\min}} & \text{for } \Delta_{\min} \leq \Delta \leq \Delta_{\max} \\ 0 & \text{for } 0 < \Delta < \Delta_{\min}, \Delta > \Delta_{\max} \end{cases} \quad (3)$$

where  $\Delta_{\min}$  and  $\Delta_{\max}$  represent the minimum and maximum gap value, respectively. The solid line in figure 5 represents the calculated differential conductance at 4.2 K with

$\Delta_{\min} = 9$  meV and  $\Delta_{\max} = 27$  meV. The essential behaviour is almost reproduced except for the observed finite conductance near zero-bias voltage. In order to fit the low-energy region well, we introduce the broadening of the one-electron level. The broken line in figure 5 is the broadened curve of the solid line in the figure with the broadening parameter  $\Gamma = 0.9$  meV. As is clear in the figure, the agreement is satisfactory. The  $\Gamma$  value of 0.9 meV is very small compared with those adopted in other tunnelling experiments. It assures the validity of the discussion for the superconducting electronic state with our tunnelling spectra. In this fitting, we used the rectangular form of  $D(\Delta)$ . However, this form is not essential, but it is important that the gap has its minimum and maximum value. It is understood that the gap is finite on the whole Fermi surface while  $\Delta$  varies from 9 to 27 meV depending on the direction in  $k$ -space. Additionally, the observed finite conductance near zero-bias voltage is presumably explained by the small broadening effect.

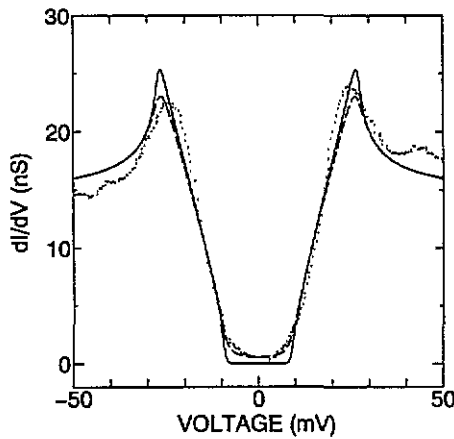


**Figure 5.** Fitting of the conductance obtained to the anisotropic model with finite gap. The solid line represents the calculated conductance for 4.2 K from the anisotropic gap model with  $\Delta_{\min} = 9$  meV and  $\Delta_{\max} = 27$  meV described in the text. The broken line represents the broadened curve of the solid line with  $\Gamma = 0.9$  meV.

If we assume that the superconductivity occurs in a two-dimensional square lattice formed by Cu and O atoms and that the interaction acts only among the nearest neighbours, the interaction of the d-wave symmetry, which gives large gap anisotropy, would be a favourable one. However, the pure d wave is excluded, as is described above. The extended s wave is another symmetry for the square lattice and also gives the gap anisotropy. For the extended s-wave symmetry with nearest-neighbour interactions in the square lattice and with lattice constant  $a$ , the gap is described simply as

$$\Delta(k) = \Delta_0 + \Delta_1(\cos(k_x a) + \cos(k_y a)) \quad (4)$$

where  $\Delta_0$  is the isotropic component and  $\Delta_1$  is the amplitude of the anisotropic component. The observed finite gap is not inconsistent with the extended s wave. However, the calculated gap anisotropy does not become large, because the electronic band dispersion is expected to have a  $k$ -dependence similar to that of the anisotropic term in equation (4). The observed large anisotropy is hardly explained by the extended s wave. Our present results suggest the contribution of the d-wave component. It is considered that the finite gap

is brought about by the s-wave component and that the d-wave component gives relatively large anisotropy. The  $s+id$  symmetry proposed by Kotliar [14], in which the order parameter does not vanish, is also a possible pairing. However, we cannot distinguish  $s+d$  from  $s+id$  at present. Our tunnelling result strongly suggests the mixed pair symmetry of s and d waves, although it is an open problem to make the origin of the mixed symmetry clear.

In summary, we investigated the cleaved surface of single crystals of  $\text{Bi}_2\text{Sr}_2\text{CaCu}_2\text{O}_8$  by low-temperature STM. The low-noise tunnelling differential conductance obtained is essentially the same as that for the lateral surface in the previous experiment. We concluded that the tunnelling current contains contributions from electrons with every wave number in the tunnelling configuration with STM. From the model calculation for an anisotropic gap, it is concluded that the gap is finite while it varies from 9 to 27 meV depending on the direction in  $k$ -space. It is suggested that the symmetry of the pair wave function is of the mixed symmetry of s and d waves.

This work was supported in part by a Grant-in-Aid for Scientific Research on Priority Areas given by the Ministry for Education, Science and Culture.

## References

- [1] Hardy W N, Bonn D A, Morgan D C, Liang R and Zhang K 1993 *Phys. Rev. Lett.* **70** 3999–4002
- [2] Shen Z X, Dessau D S, Wells B O, King D M, Spicer W E, Arko A J, Marshall D, Lombardo L W, Kapitulnik A, Dickinson P, Doniach S, DiCarlo J, Loeser A G and Park C H 1993 *Phys. Rev. Lett.* **70** 1553–6
- [3] Hammel P C, Takigawa M, Heffner R H, Fisk Z and Ott K C 1989 *Phys. Rev. Lett.* **63** 1992–5
- [4] Kane J, Chen Q, Ng K W and Tao H J 1994 *Phys. Rev. Lett.* **72** 128–31
- [5] Tanaka S, Ueda E, Sato M, Tamasaku K and Uchida S 1995 *J. Phys. Soc. Japan* **64** 1476–80
- [6] Ichimura K and Nomura K 1993 *J. Phys. Soc. Japan* **62** 3661–79
- [7] Ichimura K, Nomura K, Minami F and Takekawa S 1992 *Solid State Commun.* **82** 171–5
- [8] Manabe C, Oda M and Ido M 1994 *Physica C* **235–240** 797–8
- [9] Renner Ch and Fischer Ø 1995 *Phys. Rev. B* **51** 9208–18
- [10] Wolf E L 1989 *Principles of Electron Tunneling Spectroscopy* (New York: Oxford University Press) p 23
- [11] McMillan W L and Rowell J M 1969 *Superconductivity* ed R D Parks (New York: Marcel Dekker) p 574
- [12] Blackford B L and March R H 1969 *Phys. Rev.* **186** 397–9
- [13] Tanemoto T, Kohno H and Fukuyama H 1992 *J. Phys. Soc. Japan* **61** 1886–90
- [14] Kotliar G 1988 *Phys. Rev. B* **37** 3664–6